Cell, Vol. 94, 739–750, September 18, 1998, Copyright ©1998 by Cell Press

Apaf1 Is Required for Mitochondrial Pathways of Apoptosis and Brain Development

Hiroki Yoshida,*† Young-Yun Kong,*†
Ritsuko Yoshida,*† Andrew J. Elia,*†
Anne Hakem,*† Razqallah Hakem,*†
Josef M. Penninger,*† and Tak W. Mak*†‡
*The Amgen Institute
620 University Avenue
Toronto, Ontario
†Ontario Cancer Institute and the Departments
of Medical Biophysics and Immunology
University of Toronto
Toronto, Ontario
Canada M5G 2C1

Summary

Apoptosis is essential for the precise regulation of cellular homeostasis and development. The role in vivo of Apaf1, a mammalian homolog of *C. elegans* CED-4, was investigated in gene-targeted *Apaf1*$^{-/-}$ mice. Apaf1-deficient mice exhibited reduced apoptosis in the brain and striking craniofacial abnormalities with hyperproliferation of neuronal cells. Apaf1-deficient cells were resistant to a variety of apoptotic stimuli, and the processing of Caspases 2, 3, and 8 was impaired. However, both *Apaf1*$^{-/-}$ thymocytes and activated T lymphocytes were sensitive to Fas-induced killing, showing that Fas-mediated apoptosis in these cells is independent of Apaf1. These data indicate that Apaf1 plays a central role in the common events of mitochondria-dependent apoptosis in most death pathways and that this role is critical for normal development.

Introduction

Apoptosis or programmed cell death (PCD) is critical for the normal development of the body and occurs in many developing tissues in both invertebrates and vertebrates (Clarke and Clarke, 1996; Jacobson et al., 1997). Rationalization of cell numbers by PCD is particularly important in the developing central nervous system (CNS). Many developing vertebrate neurons are thought to compete for limiting amounts of survival signals (neurotrophic factors) secreted by the target cells they innervate (Oppenheim, 1991; Oppenheim et al., 1991). Only that small proportion of neurons receiving sufficient quantities of these signals survives, while the remaining cells undergo PCD (Barde, 1989; Oppenheim, 1991).

Apoptosis is also essential for the development and maintenance of the immune system (Nagata, 1997). Developing T lymphocytes that either fail to produce functional antigen-specific receptors or produce self-reactive receptors are eliminated by PCD in the thymus. In the periphery, self-reactive T cells as well as antigen-stimulated mature T cells are deleted by a mechanism of activation-induced cell death mediated by Fas. PCD in these situations prevents autoimmune disease and the inappropriate accumulation of lymphocytes.

Core components of the cell death machinery are conserved from nematodes to humans (Yuan et al., 1993; Hengartner and Horvitz, 1994; Zou et al., 1997). Genetic analyses of *Caenorhabditis elegans* mutants have identified two killer genes, *ced-3* and *ced-4*, and an antiapoptotic gene, *ced-9*, that are important for the regulation of cell death (Horvitz et al., 1983; Ellis and Horvitz, 1986). The *ced-9* gene is homologous to the mammalian *Bcl2* gene family, some members of which (such as *Bcl2* and *BclX*) inhibit PCD, while others (such as *Bax* and *Bak*) promote PCD. The CED-3 protein is homologous to the proapoptotic cysteine proteases known as the caspases, among which Caspase 3 (Casp3) exhibits the highest degree of similarity to CED-3 (Yuan et al., 1993; Fernandes-Alnemri et al., 1994). The caspases can be activated by a wide variety of apoptotic stimuli and mediate PCD by cleaving selected intracellular proteins, including proteins of the nucleus, nuclear lamina, cytoskeleton, endoplasmic reticulum, and cytosol, thereby disabling important cellular processes and breaking down structural components of the cell (Nicholson and Thornberry, 1997; Thornberry, 1998).

ced-4 has been determined genetically to function downstream of *ced-9* but upstream of *ced-3* (Shaham and Horvitz, 1996). APAF1, a mammalian homolog of CED-4, (Zou et al., 1997), has been shown to bind CASP9 via the caspase recruitment domain (CARD) (Hofmann et al., 1997) at its NH_2 terminus (Li et al., 1997a; Hu et al., 1998; Pan et al., 1998). In vitro, in the presence of cytochrome c and dATP, this interaction leads to the activation of CASP9 and the subsequent proteolytic activation of CASP3 (Li et al., 1997a). Like CED-4, which has been shown to participate in a ternary complex with CED-9 and CED-3 (Chinnaiyan et al., 1997; Spector et al., 1997; Wu et al., 1997a, 1997b), APAF1 forms a complex with $BclX_L$ and CASP9 (Hu et al., 1998; Pan et al., 1998). Although the roles in PCD of Bcl2 family members, cytochrome c, and the caspases have been extensively studied, little is known about the function of the key intermediary molecule Apaf1.

To investigate the biological function of Apaf1 in vivo, we generated *Apaf1*$^{-/-}$ null-mutant mice. Analyses of *Apaf1*$^{-/-}$ mice in vivo as well as ex vivo suggest that Apaf1 is essential for the normal development of the CNS during embryogenesis. Our results also show that Apaf1 is a central element in the mitochondrial pathways of PCD induced in response to a wide range of apoptotic stimuli, but that Fas-mediated PCD in thymocytes and activated T cells is independent of Apaf1.

Results

Generation of *Apaf1*$^{-/-}$ Mutant Mice

The *Apaf1* gene was disrupted in murine embryonic stem (ES) cells using a targeting vector in which an exon encoding a portion of the nucleotide-binding P loop was deleted (see Experimental Procedures and Figure 1A).

‡To whom correspondence should be addressed.

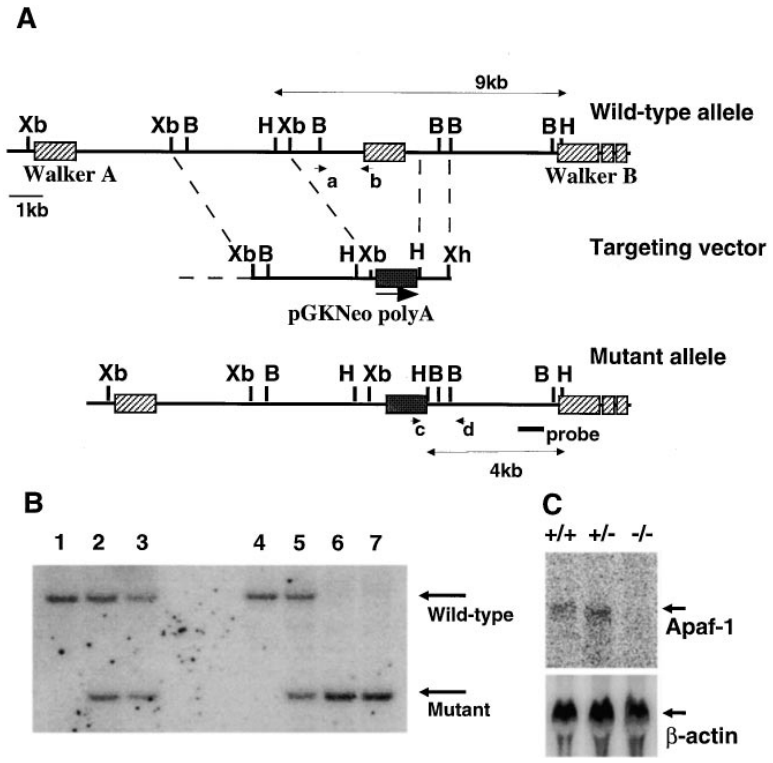

Figure 1. Targeted Disruption of the *Apaf1* Locus

(A) A portion of the mouse *Apaf1* wild-type locus (top) showing exons (hatched boxes) and a 9.0 kb HindIII fragment in the wild-type allele. The targeting vector (middle) was designed to replace an exon encoding a portion of the nucleotide-binding domains with a neomycin resistance gene (closed box). The mutated *Apaf1* locus (bottom) contains a 4.0 kb HindIII fragment. The position of the 3′ flanking probe used for Southern blot analysis is shown. Positions of PCR primers for the wild-type allele (a and b) and the mutant allele (c and d) are also shown. Xb, B, H, and Xh represent XbaI, BamHI, HindIII, and XhoI sites, respectively.

(B) Southern blot analysis of wild-type and mutant ES cell DNA. Genomic DNA from wild-type ES cells (lanes 1 and 4), three independent *Apaf1*$^{+/-}$ ES cell clones (lanes 2, 3, and 5), and two *Apaf1*$^{-/-}$ ES cell clones (lanes 6 and 7) were digested with HindIII and hybridized to the 3′ flanking probe. The 9 kb wild-type fragment and the 4 kb mutant fragment are indicated.

(C) Northern blot analysis of *Apaf1* expression. Total RNA extracted from E9.5 embryos (20 μg/lane) was analyzed for the expression of *Apaf1* gene.

The targeting vector was electroporated into ES cells. Three G418-resistant colonies were found to be heterozygous for the mutation at the *Apaf1* locus (Figure 1B). The heterozygous mutant ES cells were used to generate chimeric mice. Chimeras were backcrossed to strains C57BL/6 or CD1 to generate mice heterozygous for the *Apaf1* mutation. Heterozygous *Apaf1*$^{+/-}$ mice were healthy and fertile and were intercrossed to generate homozygous *Apaf1*$^{-/-}$ mice. The null mutation of *Apaf1* was confirmed by the absence of *Apaf1* expression as determined by Northern blot analysis of RNA extracted from embryos on day 9.5 of gestation (E9.5) (Figure 1C). *Apaf1*$^{-/-}$ ES cells were also established to generate the *Apaf1*$^{-/-}$/*Rag1*$^{-/-}$ chimeric mice (Figure 1B).

Perinatal Lethality of *Apaf1*$^{-/-}$ Mutant Mice

Of 190 offspring derived from heterozygous matings, 11 homozygous *Apaf1*$^{-/-}$ mutants were identified (Table 1). However, all but three *Apaf1*$^{-/-}$ mice were found dead at birth or died within 12 hr after birth. To determine the stage of embryonic development affected by the *Apaf1* mutation, timed breedings followed by embryo genotyping were performed. From E11.5 to E16.5, *Apaf1*$^{-/-}$ embryos were viable, usually of normal size, and occurred at the expected Mendelian frequency. However, at E12.5 and thereafter, most *Apaf1*$^{-/-}$ embryos showed morphological abnormalities: (a) ectopic masses on the forehead; (b) a cauliflower-like mass on the face; and (c) a cone-shaped head mass with exencephalus. These three phenotypes were observed at similar frequencies, and the genetic background of mice (C57BL/6 or CD1) did not affect the ratio.

Apaf1 Gene Expression in the Embryo and Adult Tissues

The spatial distribution of *Apaf1* gene expression in wild-type embryos was analyzed by in situ hybridization. At E9.5, *Apaf1* mRNA was strongly expressed in the developing hindbrain and in the regions lining the third ventricle at the basal telencephalon and diencephalon, and it was weakly expressed along the entire length of the mesencephalon and telencephalon (Figures 2A and 2B). At E12.5 to 14.5, a low level of *Apaf1* expression was observed ubiquitously throughout the wild-type embryo (data not shown). The expression of *Apaf1* was also confirmed in wild-type ES cells, thymocytes, and splenocytes by RT-PCR analysis (data not shown).

Histological Analyses of Structural Abnormalities in *Apaf1*$^{-/-}$ Mutant Embryos

The structural abnormalities of *Apaf1*$^{-/-}$ mutants were characterized by histological analyses of serially sectioned E12.5-E16.5 embryos. Examination of sections from mutant mice with ectopic masses on the forehead (Figure 3A; phenotype a) revealed that the protrusions were an extension of the forebrain (Figure 3C). These extensions showed remarkable thickening of the mitotic ventricular zone, although the normal layered organization of the forebrain was maintained (Figure 3C, inset). In newborn *Apaf1*$^{-/-}$ mice, the forebrain masses were hemorrhagic and necrotic (data not shown). Nevertheless, these types of forebrain masses constituted the least severe mutant phenotype, because the overall cytoarchitectural structure of the brain was relatively intact, and the three *Apaf1*$^{-/-}$ mice that survived until 10 days after birth were of this phenotype.

Table 1. Genotype Analysis of the Progeny from *Apaf1* Heterozygous Intercrosses

Stage	No. of the Genotypes (Percentage)			†Phenotype	Total
	+/+	+/−	−/−	(a, b, c, n)	
E11.5	4 (20)	10 (50)	6 (30)	(0, 0, 0, 6)	20
E12.5	8 (29)	14 (50)	6 (21)	(1, 1, 1, 3)	28
E13.5	14 (26)	23 (43)	16 (30)	(4, 5, 5, 2)	53
E14.5	15 (27)	28 (51)	12 (22)	(3, 4, 4, 1)	55
E15.5	11 (25)	20 (45)	13 (30)	(4, 4, 5, 0)	44
E16.5	16 (38)	14 (33)	12 (29)	(7, 3, 2, 0)	42
E18.5	10 (27)	20 (56)	6 (17)	(3, 2, 1, 0)	36
Newborn	63 (33)	116 (61)	*11 (6)	(7, 2, 2, 0)	190
Total					468

Timed breedings were performed with *Apaf1* heterozygous intercrosses. The day when females were plugged was defined as E0.5.
† Phenotype a, forehead masses; b, a face mass; c, a cone-shaped mass; and n, no obvious anomaly (See text).
* Three mutants with masses on the forehead survived up to day 10 after birth.

In mutant embryos with a cauliflower-like mass on the face and a small, flat head (Figures 3D; phenotype b), striking deformities of the thalamus, hypothalamus, and forebrain were observed (compare Figures 3F and 3G with the wild type in 3E). The thalamic areas of the mutant embryos were filled with supernumerary cells, producing a wedge-shaped deformation (Figure 3F). The cauliflower-like mass on the face stained positively for neurofilament light chain (data not shown), thus identifying it histologically to be forebrain tissue. This mass exhibited significant thickening of the cortex but a normal layering pattern (data not shown). Significant hyperplasia of the choroid plexus of these animals was also observed.

In *Apaf1*$^{-/-}$ embryos with a cone-shaped head mass and exencephalus (Figure 3H; phenotype c), ectopic masses were observed (Figure 3I; asterisk), probably resulting from an overgrowth of the thalamus and hypothalamus. Mutants of this phenotype also displayed a remarkably extended hindbrain (Figure 3I, inset).

The primary cause of death of most *Apaf1*$^{-/-}$ embryos appeared to be mechanical disruption of the brain masses during delivery, since most mutants appeared viable and were found at the expected Mendelian frequency when dissected (Table 1). However, because the frequency of *Apaf1*$^{-/-}$ embryos at E18.5 was already lower than that predicted by Mendelian genetics, some mutants, especially those with phenotypes b and c, appeared to die before birth (Table 1), possibly succumbing to secondary effects such as hydrocephalus.

TUNEL assays were used to examine apoptosis in the brains of mutant and wild-type embryos. Numerous TUNEL-positive cells indicating the presence of apoptotic nuclei were observed in the hindbrain of E14.5 wild-type embryos (Figure 3J), whereas fewer TUNEL-positive cells were detected in the corresponding area of the mutant embryo (Figure 3K; phenotype c). The mutant embryos also exhibited reduced apoptosis in the roof of the midbrain and the cortex of the forebrain (both in embryos with phenotype b and c) at E14.5 (data not shown). Other areas, such as mesenchymal tissue in the brain, showed no difference in PCD (data not shown). These results demonstrate that apoptosis was dramatically reduced in the developing brain of *Apaf1*$^{-/-}$ embryos.

The supernumerary cells in the thalamic areas of phenotype b or in the ectopic mass of phenotype c (Figures 3G and 3I, asterisks) showed increased mitotic activity at E14.5 compared to the control as determined by BrdU incorporation (data not shown). However, by E16.5, BrdU incorporation had ceased in these areas (data not shown), suggesting that the supernumerary cells were not proliferating tumors. The increased BrdU incorporation in the mutant embryos was detected in other areas, such as in the hindbrain at E12.5 and in the forebrain at E13.5 (Figures 3L–3O). Mutant embryos exhibited higher labeling index (labeled nuclei per total nuclei) than wild-type littermates: 15.7% ± 2.9% vs. 10.1% ± 1.1% in the hindbrain at E12.5 and 40.2% ± 5.8% vs. 19.9% ± 4.8% in the forebrain at E13.5; mutant versus wild type.

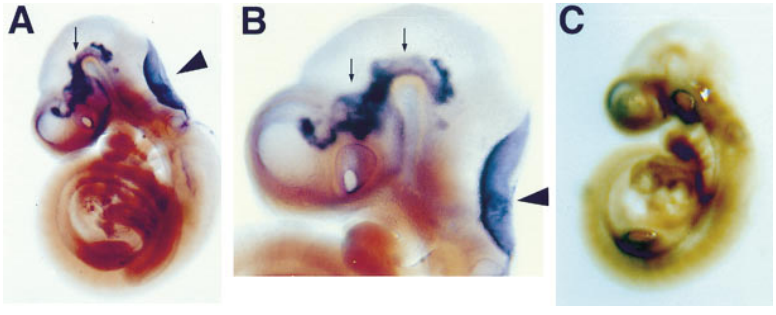

Figure 2. Expression of *Apaf1* in the Brain of a Wild-Type Embryo

(A) Whole-mount in situ hybridization of an E9.5 wild-type embryo. *Apaf1* expression (purple) was strongly detected in the region of the developing hindbrain (arrowhead). The expression was also detected in the basal telencephalon and diencephalon (arrows). Weak expression was detected ubiquitously along the mesencephalon and the remainder of telencephalon. Original magnification, 40×.
(B) Higher power view of the same embryo. Original magnification, 64×.
(C) Negative control: no signal was detected with a probe in a sense orientation.

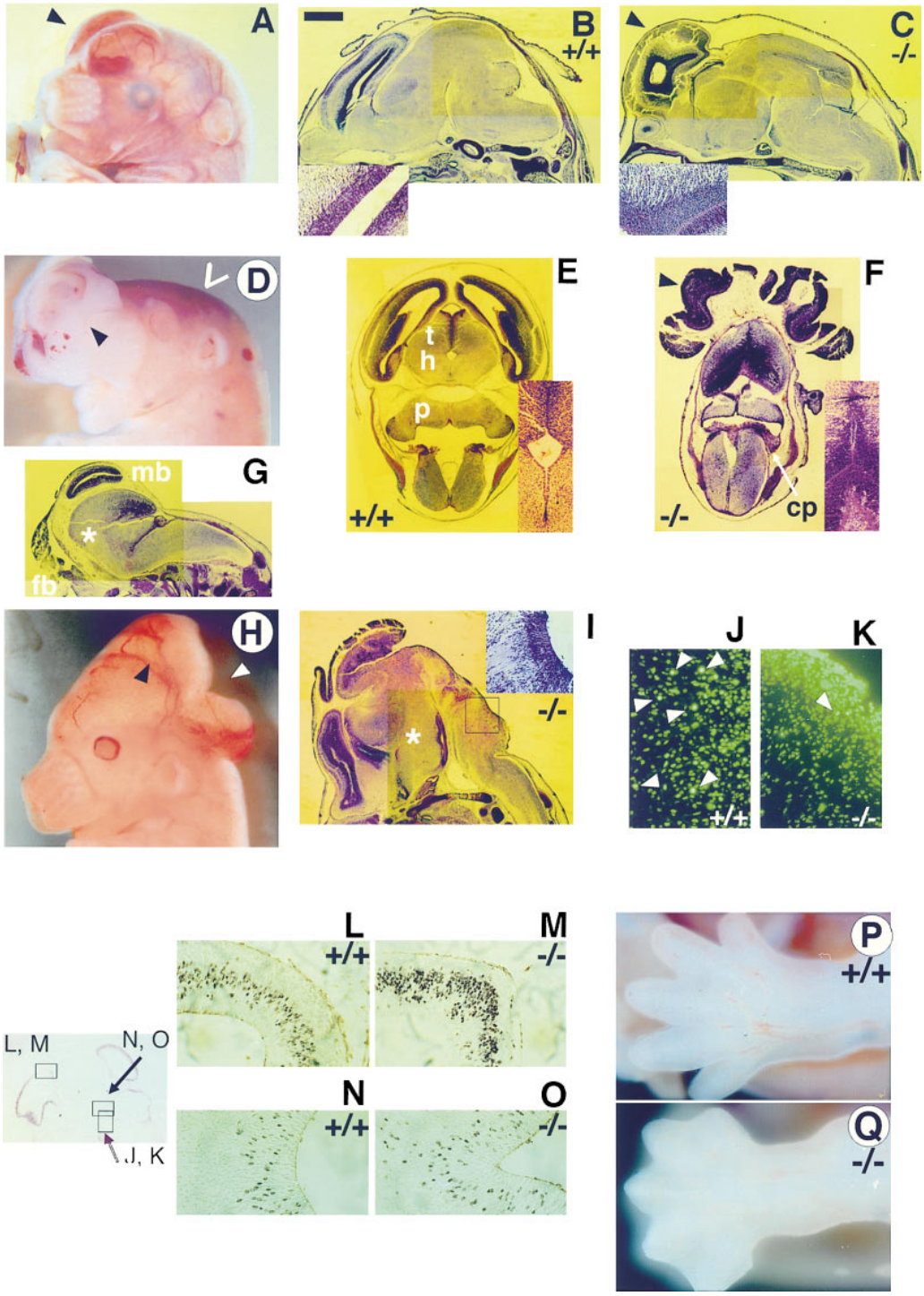

Figure 3. Phenotypes of *Apaf1*$^{-/-}$ Embryos

(A) Protrusion of brain tissue on the frontal bone area (arrowhead) at E15.5.

(B and C) Cytoarchitectural organization of wild-type (B) and mutant (C) mice at E16.5; parasagittal section. An arrowhead shows the protrusion of forebrain with thickening of the cortex. Insets show high-power views of the forebrains; the normal layered pattern observed in wild-type mice is maintained in mutant mice. Bar, 500 μm.

(D) Craniofacial abnormality with a cauliflower-like mass on the face (arrowhead) and small head (chevron) of an *Apaf1*$^{-/-}$ embryo at E14.5.

(E and F) Horizontal views of wild-type (E) and *Apaf1*$^{-/-}$ (F) embryos at E14.5 showing the wedge-shaped deformity of thalamus and hypothalamus with supernumerary cells in the mutant. Remarkable thickening of forebrain (arrowhead) and hyperproliferation of the choroid plexus (cp) in the mutant can also be seen. t, thalamus; h, hypothalamus; and p, pons. Insets show the third ventricles; the third ventricle in the mutant shows complete occlusion.

(G) A sagittal view of an *Apaf1*$^{-/-}$ embryo at E14.5. The abnormally shaped thalamic area with the head deformity is prominent (asterisk). mb, midbrain; fb, forebrain.

A Delay in Removal of Interdigital Webs in *Apaf1*$^{-/-}$ Mutant Embryos

The formation of digits in higher vertebrate species is a well-studied example in which PCD eliminates the cells between developing digits (Jacobson et al., 1996). *Apaf1*$^{-/-}$ embryos showed poorly shaped digits with a delay in the removal of interdigital webs of forelimbs at E13.5 (4 out of 16) and of hindlimbs at E14.5 (4 out of 12) (Figure 3Q and data not shown). However, at E15.5 and later, apparently normal development of digits and removal of interdigital webs were seen in all mutant embryos.

Resistance of *Apaf1*$^{-/-}$ ES Cells and Embryonic Fibroblasts to Various Apoptotic Stimuli

To investigate the role of Apaf1 in PCD of various cell types, we examined the susceptibility of *Apaf1*$^{-/-}$ ES and embryonic fibroblast (EF) cells to apoptotic stimuli. Apoptosis of *Apaf1*$^{+/-}$ and *Apaf1*$^{-/-}$ ES cells was induced by treatment with either anisomycin, cisplatinum, etoposide, or UV irradiation. Six or 24 hr after induction of PCD, cells were evaluated for apoptotic cell death by propidium iodide (PI) staining and annexin V costaining. Annexin V staining detects the loss of cell membrane phospholipid asymmetry; in particular, phosphatidylserine becomes exposed to the outer membrane during the early phases of apoptosis (Fadok et al., 1992). Although a low level of cell death occurred after UV irradiation, *Apaf1*$^{-/-}$ ES cells were generally protected from PCD induced by all stimuli tested (Figure 4A). Moreover, there was virtually no increase in the annexin V-positive population in *Apaf1*$^{-/-}$ ES cells following stimulation.

We also examined the susceptibility of primary EF cells to apoptotic stimuli (Figure 4B). Compared to heterozygous EF cells, *Apaf1*$^{-/-}$ EF cells were also protected from PCD induced by all stimuli tested, although they were not as resistant as *Apaf1*$^{-/-}$ ES cells. A substantial increase in the proportion of *Apaf1*$^{-/-}$ EF cells staining positively for annexin V was observed. The difference in degree of resistance to apoptotic stimuli between *Apaf1*$^{-/-}$ ES and EF cells suggests a differential requirement for Apaf1 in the apoptotic machinery of different cell types.

Cytochrome c Release Is Not Impaired in *Apaf1*$^{-/-}$ EF Cells

Cytochrome c is required for the APAF1-mediated proteolytic activation of CASP9 (Li et al., 1997a). We examined the effect of Apaf1 on cytochrome c release from mitochondria by immunofluoresence microscopy in EF cells (Figure 4C). In both *Apaf1*$^{+/-}$ and *Apaf1*$^{-/-}$ untreated EF cells, cytochrome c displayed punctate staining pattern consistent with its localization in mitochondria. Following stimulation with etoposide, staurosporine, or UV irradiation, both *Apaf1*$^{+/-}$ and *Apaf1*$^{-/-}$ EF cells exhibited mostly diffuse cytoplasmic cytochrome c staining, consistent with its translocation from mitochondria to cytoplasm (Bossy-Wetzel et al., 1998). Thus the release of cytochrome c is not impaired in *Apaf1*$^{-/-}$ EF cells in response to these stimuli, suggesting that Apaf1 acts downstream of cytochrome c release.

Apaf1$^{-/-}$ Thymocytes Are Resistant to Various Apoptotic Stimuli but Sensitive to Fas-Mediated Killing

Since PCD plays a critical role in thymocyte selection, we investigated whether the Apaf1-mediated apoptotic pathway was involved in the development of thymocytes. Thymic development was examined in three *Apaf1*$^{-/-}$ mice that had survived until 10 days of age. Thymi from *Apaf1*$^{-/-}$ mice yielded fewer thymocytes ($90 \pm 12 \times 10^6$) than heterozygous ($230 \pm 30 \times 10^6$) littermates, but this number was proportional to the smaller body size of the mutants. Flow cytometric analyses of *Apaf1*$^{-/-}$ thymocytes revealed normal development of CD4$^+$ and CD8$^+$ cells (data not shown). Normal thymocyte development in the absence of Apaf1 was also confirmed in *Apaf1*$^{-/-}$/*Rag1*$^{-/-}$ chimeric mice (data not shown). Therefore, the apoptotic pathway required for normal thymocyte development does not require Apaf1.

We then examined the susceptibility of *Apaf1*$^{-/-}$ thymocytes to various apoptotic stimuli. In contrast to *Casp3*$^{-/-}$ thymocytes, but similar to *Casp9*$^{-/-}$ thymocytes (Kuida et al., 1996, 1998; Hakem et al., 1998; Woo et al., 1998), *Apaf1*$^{-/-}$ thymocytes were resistant to a wide range of apoptotic stimuli, particularly dexamethasone (Dex), etoposide, and γ-irradiation (Figures 5A and 5B). However, *Apaf1*$^{-/-}$ thymocytes showed normal susceptibility to Fas-mediated cell death, demonstrating that Apaf1 is dispensable for the Fas-mediated apoptotic pathway in thymocytes.

Activated *Apaf1*$^{-/-}$ Peripheral T Cells Are Resistant to UV Irradiation but Sensitive to Fas-Mediated Killing

To determine the involvement of Apaf1 in the PCD of activated peripheral T cells, the response of these cells to treatment with UV irradiation or Fas ligation was examined. Equal numbers of heterozygous and homozygous cells were killed by Fas ligation (percentages of viable cells remaining were 71.4% ± 3.0% and 65.0% ± 4.0% at 6 hr, and 46.0% ± 4.9% and 38.1% ± 4.2% at

(H) An *Apaf1*$^{-/-}$ mutant (E13.5) showing a cone-shaped mass on the head (arrowhead) and exencephalus (white arrowhead).
(I) A sagittal view of an *Apaf1*$^{-/-}$ embryo (E14.5) showing an ectopic mass (asterisk) and extended hindbrain. Inset, a high-power view of the area in the square showing a ventricular zone exposed outside due to the extended hindbrain.
(J and K) TUNEL assay showing the reduced apoptosis in the *Apaf1*$^{-/-}$ mutant ([K]; phenotype c) compared with that in the wild type ([J], arrowheads). Areas of the hindbrain in sagittally cut sections (E14.5) were stained for apoptotic nuclei.
(L–O) BrdU incorporation in brains of wild-type and *Apaf1*$^{-/-}$ embryos. Areas in the forebrain of wild-type (L) and mutant ([M]; phenotype b) at E13.5 and areas in the hindbrain of wild-type (N) and mutant ([O]; phenotype b) at E12.5 are shown.
Original magnifications: (B), (C), (E)–(G), and (I), 25×; (J) and (K), 400×; (L)–(O), 200×.
The frontal mass in (D) and the rostral mass in (H) are assumed to be lost during delivery.
(P and Q) Delayed removal of interdigital webs in *Apaf1*$^{-/-}$ embryos. Hind limb of wild-type (P) and *Apaf1*$^{-/-}$ mutant (Q) embryos at E14.5 showing a delay in the removal of the interdigital webs in the mutant.

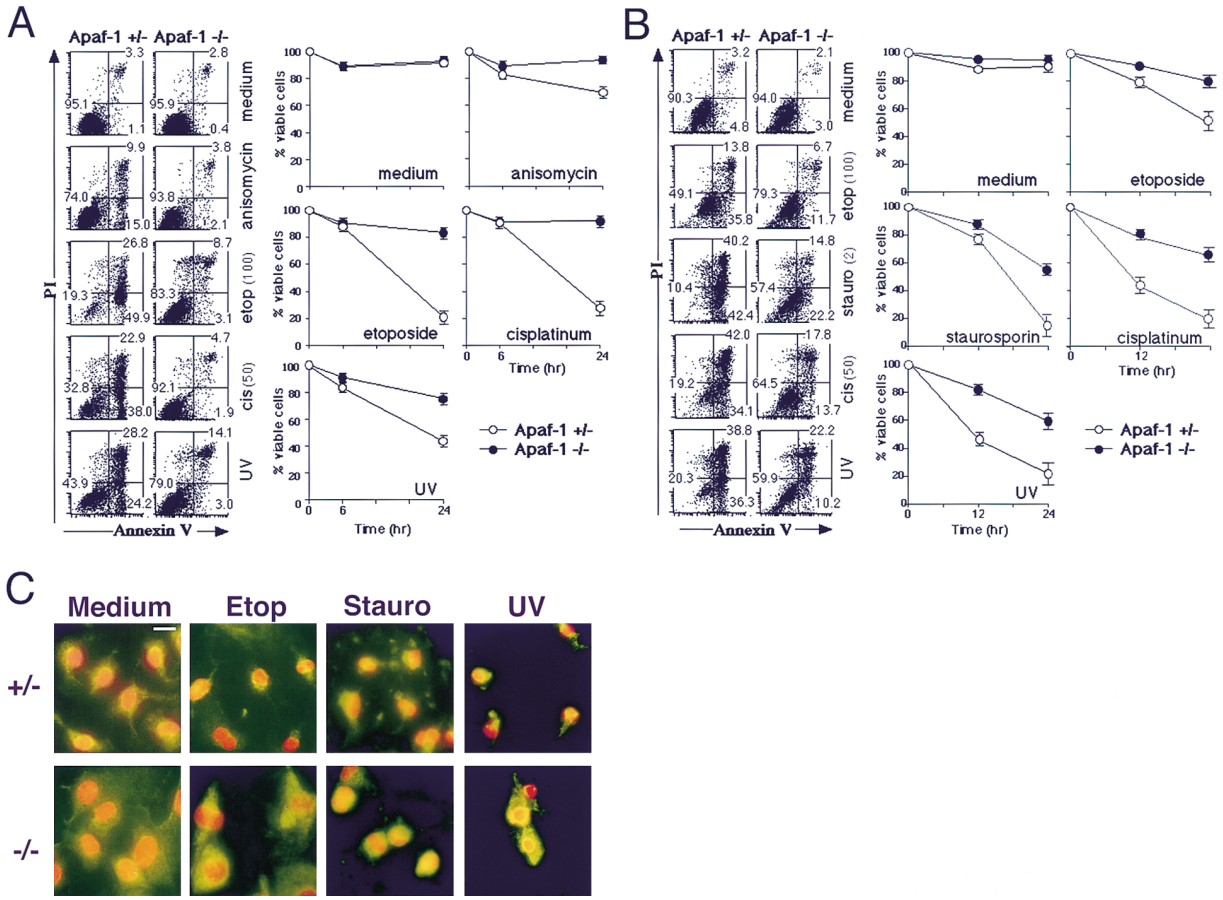

Figure 4. Resistance of *Apaf1*$^{-/-}$ ES and EF Cells to Various Apoptotic Stimuli

(A) Resistance of *Apaf1*$^{-/-}$ ES cells. *Apaf1*$^{+/-}$ and *Apaf1*$^{-/-}$ ES cells were stimulated for the induction of apoptosis and evaluated for cell death as described in Experimental Procedures. Data from inductions with anisomycin, etoposide (100 μM), cisplatinum (50 μM), and UV irradiation are shown.

(B) Resistance of *Apaf1*$^{-/-}$ EF cells. EF cells were stimulated as in (A). Data from stimulations with etoposide (100 μM), staurosporine (2 μM), cisplatinum (50 μM), and UV irradiation are shown.

(Left) annexin V vs. PI staining after 24 hr treatment with apoptotic stimuli. Number in each panel represents the percentage of cells in that quadrant.

(Right) Cell viability after induction of apoptosis. The percentages of viable cells (annexin V–negative and PI-negative cell population) after stimulation are shown. The figures show data representative of three independent experiments.

(C) Cytochrome c release visualized by immunofluorescence microscopy.

Intracellular localization of cytochrome c (green) and nuclear morphology (red) is shown in untreated, etoposide-, staurosporine-, and UV-treated EF cells. Top, *Apaf1*$^{+/-}$; bottom, *Apaf1*$^{-/-}$ EF cells. Bar, 20 μm.

12 hr, heterozygous and homozygous mutant, respectively). However, significantly more heterozygous cells underwent PCD in response to UV irradiation than did homozygous mutant cells (8.8% ± 1.0% vs. 27.4% ± 5.0% viable cells at 6 hr). Thus, activated *Apaf1*$^{-/-}$ peripheral T cells are resistant to UV irradiation to some degree, but Apaf1 is dispensable for Fas-mediated cell death in activated peripheral T cells.

Resistance to the Loss of Mitochondrial Transmembrane Potential ($\Delta\Psi_m$) in *Apaf1*$^{-/-}$ Thymocytes

To explore further the mechanism of resistance to apoptosis in *Apaf1*$^{-/-}$ cells, the potential-sensitive dye 3, 3′-dihexyloxacarbocyanine iodide ($DiOC_6(3)$) (Petit et al., 1995) was used to evaluate changes in the mitochondrial transmembrane potential ($\Delta\Psi_m$) following the induction of apoptosis in thymocytes. As expected, the loss of $\Delta\Psi_m$ in response to Fas-mediated killing was similar in *Apaf1*$^{-/-}$ and control thymocytes (Figure 5C), confirming that the Fas-mediated apoptotic pathway is independent of Apaf1. However, $\Delta\Psi_m$ was maintained in the *Apaf1*$^{-/-}$ thymocytes compared with control thymocytes in response to other apoptotic stimuli. This result suggests that *Apaf1*$^{-/-}$ thymocytes are protected not only from apoptotic death but also from mitochondrial changes and indicates that Apaf1 lies upstream of these apoptotic changes as exemplified by the loss of $\Delta\Psi_m$.

Activation of Casp2, Casp3, and Casp8 in *Apaf1*$^{-/-}$ Thymocytes

To determine the consequences of the *Apaf1* mutation on the caspase cascade, we examined the activation of Casp3 in *Apaf1*$^{-/-}$ thymocytes (Figure 6A). As expected, the activation of Casp3 as demonstrated by the cleavage of its procaspase form was equivalent in mutant and

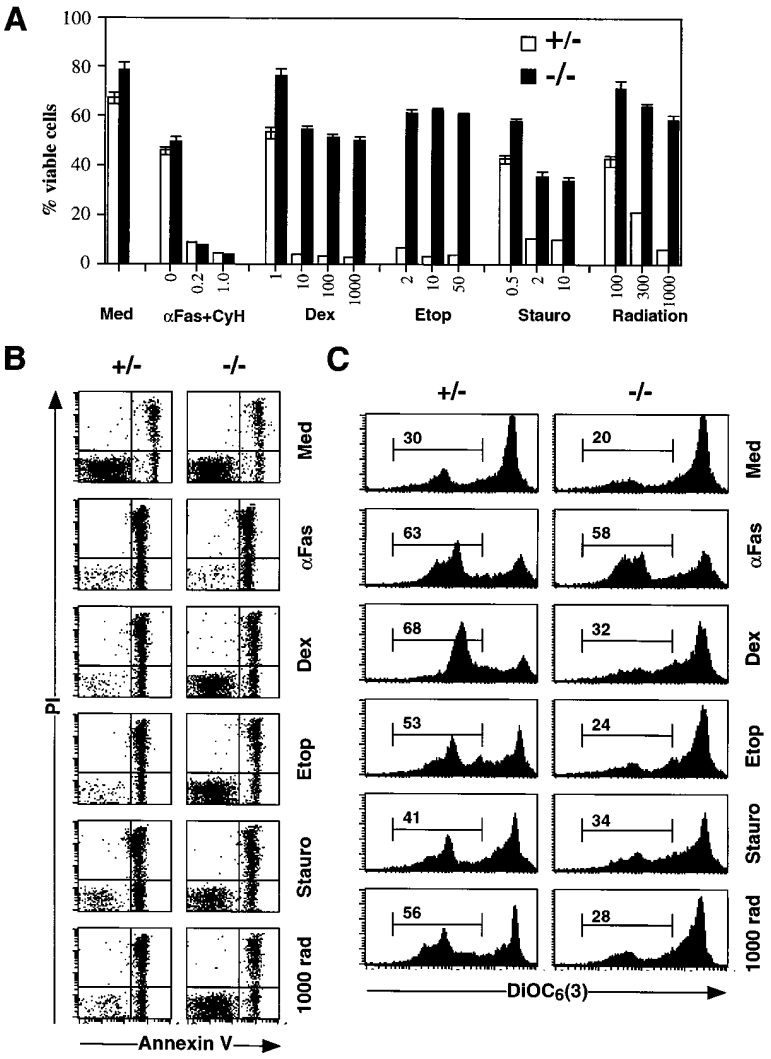

Figure 5. Resistance of *Apaf1*$^{-/-}$ Thymocytes to Various Apoptotic Stimuli

(A and B) Thymocytes from *Apaf1*$^{-/-}$ or *Apaf1*$^{+/-}$ mice were stimulated with apoptotic stimuli, anti-Fas antibody (1.0 μg/ml) plus cycloheximide (CyH; 0–1.0 μg/ml), dexamethasone (1–1000 nM), etoposide (2–50 μM), staurosporine (0.5–10 μM), and γ-irradiation (100–1000 rad), as described in Experimental Procedures. Apoptotic cell death was evaluated by annexin V vs. PI staining 20 hr after stimulation. Experiments were repeated three times in triplicate using newborn *Apaf1*$^{-/-}$ or *Apaf1*$^{-/-}$/*Rag1*$^{-/-}$ chimeric mice with similar results. (A) shows the mean ± SD.

(C) Resistance to the loss of mitochondrial transmembrane potential in *Apaf1*$^{-/-}$ thymocytes. Thymocytes from *Apaf1*$^{-/-}$ and control mice were left untreated or treated with apoptotic stimuli as above. The loss of mitochondrial transmembrane potential ($\Delta\Psi_m$) was evaluated by $DiOC_6(3)$ staining 6 hr after stimulation. The number in each panel shows the percentage of the cell population exhibiting a low transmembrane potential.

(B) and (C) show the data from stimulations with anti-Fas antibody plus CyH (1 μg/ml), Dex (1000 nM), etoposide (50 nM), staurosporine (10 nM), and γ-irradiation (1000 rad).

control thymocytes in response to Fas ligation (right panel, "Fas" lanes), consistent with the finding that Casp3 can be activated independently of mitochondrial activation in Fas-induced apoptosis (Scaffidi et al., 1998). In contrast, when Dex or etoposide was used to induce PCD, the activation of Casp3 was greatly reduced compared to controls ("Dex" and "Etop" lanes), correlating with the observed maintenance of $\Delta\Psi_m$ and cell death (Figure 5) and demonstrating that Casp3 is indeed regulated downstream of Apaf1.

To determine whether the absence of Apaf1 affects the activation of other caspases, we examined the proteolytic processing of proCasp8 and proCasp2. The proteolytic activation of Casp8 was greatly reduced in *Apaf1*$^{-/-}$ thymocytes stimulated with Dex or etoposide (Figure 6B), suggesting that Apaf1 can indeed affect the activation of Casp8 in response to these stimuli. In contrast, proCasp8 processing was not impaired in *Apaf1*$^{-/-}$ thymocytes after anti-Fas antibody treatment, indicating that Casp8 activation in response to Fas stimulation can be independent of Apaf1. The activation of Casp2 was also reduced in *Apaf1*$^{-/-}$ thymocytes stimulated with Dex (Figure 6C). Moreover, p12, the active subunit derived from p14 (Li et al., 1997b), was not detected in Dex-treated *Apaf1*$^{-/-}$ thymocytes. Like the processing of Casp3 and Casp8, Casp2 cleavage was unimpaired during Fas-mediated cell death in *Apaf1*$^{-/-}$ thymocytes. Although not the only possible explanation, these results would be consistent with a scheme in which Casp8 and Casp2 are regulatory targets downstream of Apaf1. In any case, it is clear that the Fas-mediated apoptotic pathway is able to activate these caspases independently of Apaf1.

Discussion

The Role of Apaf1 in the Development of the Embryo

In this study, we have generated a null mutation of the *Apaf1* gene in mouse ES cells. The *Apaf1* mutation had a striking effect on the development of the brain during embryogenesis that resulted in perinatal lethality. Mutant embryos showed increase in the number of proliferating cells concomitant with markedly reduced apoptosis in the affected areas. The mutation also appeared to affect the development of digits.

Apoptosis determines the cytoarchitecture of the mature CNS to a significant degree (Blaschke et al., 1996; Weller et al., 1997). Recent studies on the rate of cortical

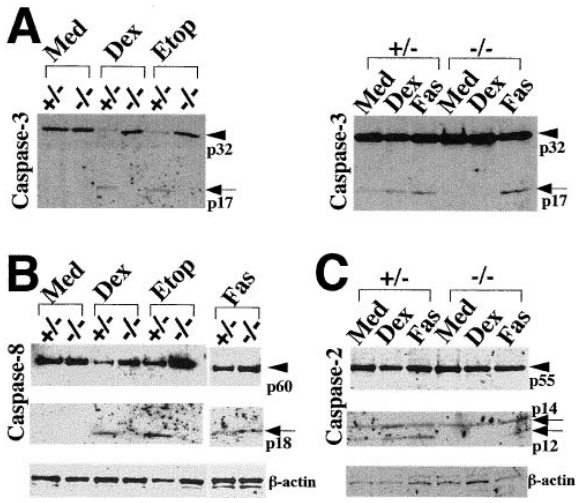

Figure 6. Caspase Activation in *Apaf1*$^{-/-}$ Thymocytes

Western blot analysis of the proteolytic activation of caspases in *Apaf1*$^{-/-}$ thymocytes. Thymocytes were either left untreated in medium (Med) or were stimulated with anti-Fas antibody (Fas; 1.0 μg/ml), dexamethasone (Dex; 1 μM, left panels or 5 nM, right panels), or etoposide (Etop; 10 μM). Protein lysates were prepared 6 hr after stimulation and Western-blotted as described in Experimental Procedures.

(A) Activation of Casp3. Proteolytic cleavage of the p32 form of Casp3 was absent after dexamethasone or etoposide treatment of *Apaf1*$^{-/-}$ thymocytes (left panel) but present after anti-Fas antibody treatment (right panel).

(B) Activation of Casp8. Cleavage of Casp8 was reduced in *Apaf1*$^{-/-}$ thymocytes treated with either dexamethasone or etoposide.

(C) Activation of Casp2. Cleavage of Casp2 to the p14 and p12 forms was reduced in *Apaf1*$^{-/-}$ thymocytes treated with dexamethasone but detected when *Apaf1*$^{-/-}$ cells were induced with anti-Fas antibody.

The β-actin blots are shown as internal controls. Arrowheads indicate the procaspases forms, and arrows indicate the processed forms of each caspase.

neurogenesis have indicated that cell production increases exponentially during brain development (Caviness et al., 1995; Takahashi et al., 1995). However, the newly produced neurons undergo PCD unless they are stimulated by nerve growth factor (NGF) released by their target cells (Blaschke et al., 1996). This dependence on limiting amounts of target cell–derived survival signals is believed to be a mechanism for matching the number of neurons to the number of target cells that need to be innervated, thus eliminating those neurons connecting to inappropriate target cells (Jacobson et al., 1997).

Consistent with this view, mice with a targeted disruption of *Casp3*, *Casp9*, or *Apaf1* die perinatally with an excess of cells in CNS and decreased PCD of neuroepithelial cells (Kuida et al., 1996, 1998; Cecconi et al., 1998 [this issue of *Cell*], Hakem et al., 1998, and this report). These mutants exhibit similar gross anatomical phenotypes, such as the protrusion of brain tissue at the frontal bone area (Figure 3A). These findings are consistent with a scenario that newly generated neurons within the ventricular zones, most of which should normally die while migrating toward superficial location, fail to undergo PCD but proliferate, resulting in the abnormal survival and accumulation of the cells, as demonstrated by the increased BrdU-positive cells and a vast excess of neural cells in the mutant (Figure 3). Thus, Apaf1, Casp9, and Casp3 act in line in a common apoptotic pathway of developing CNS, as has been demonstrated in vitro (Li et al., 1997a; Zou et al., 1997). However, *Apaf1*$^{-/-}$ mice were more drastically affected than *Casp3*$^{-/-}$ or *Casp9*$^{-/-}$ mice in terms of the extent of the affected areas in the brain and the severity of the brain deformity. For example, mutant mice with ectopic masses on the forehead, most often observed in *Casp3*$^{-/-}$ and *Casp9*$^{-/-}$ embryos, appeared to be the least severe mutant phenotype among *Apaf1* mutant embryos. Moreover, the phenotype of a cauliflower-like mass on the face (Figure 3D) was not observed in either *Casp3*$^{-/-}$ or *Casp9*$^{-/-}$ embryos. These differences raise the possibility that additional caspase(s) may also be regulated by Apaf1 during apoptosis in the brain. The observation that the delay in the removal of interdigital webs (Figure 3Q) has not been observed in either *Casp3* or *Casp9* mutant embryos also supports this possibility. Interestingly, although *Apaf1* is expressed ubiquitously in embryos at the later stages of development (Zou et al., 1997, and data not shown), the mutant phenotypes are most obvious in those areas of the brain (hindbrain and thalamic areas) where *Apaf1* is strongly expressed (E9.5). This restricted phenotype implies that other Apaf1-like molecule(s) exist that play equivalent roles in the development of other organs and tissues as well as in other areas of the brain. This hypothesis is also supported by the considerable variation in the severity of the phenotypes of *Apaf1*$^{-/-}$ mice and by the fact that an initial deficit in digit development in the mutants was overcome at later stages of development.

The Role of Apaf1 in the Immune System

Apoptosis is also critical for immune system development and homeostasis. In the thymus, the processes of positive and negative thymocyte selection exerted by the surrounding stroma result in the PCD of over 97% of developing thymocytes (Shortman et al., 1990; Surh and Sprent, 1994). In the periphery, Fas-mediated PCD eliminates self-reactive lymphocytes and controls the expansion of antigen-stimulated T cells (Nagata, 1997). However, despite the involvement of PCD in thymic selection, there were no obvious abnormalities in thymocyte development in either newborn *Apaf1*$^{-/-}$ or *Apaf1*$^{-/-}$/*Rag1*$^{-/-}$ chimeric mice. Apaf1 thus appears to be dispensable for the apoptotic pathway regulating thymocyte development, although an impairment of negative selection has not yet been ruled out.

Apaf1-deficient thymocytes failed to undergo apoptosis after treatment with various apoptotic stimuli, including etoposide, γ-irradiation, and dexamethasone. Activated *Apaf1*$^{-/-}$ peripheral T cells were also more resistant to PCD induced by UV irradiation than control cells. In contrast, the Fas-mediated apoptotic pathway was intact in both mutant thymocytes and activated peripheral T cells, demonstrating that Apaf1 is dispensable for Fas-induced PCD in these cells. In Fas-induced PCD pathways, Casp8 is activated by the formation of a death-inducing signaling complex followed by Casp3

activation (Muzio et al., 1996; Medema et al., 1997). This Fas-induced activation of Casp8 is devoid of proapoptotic mitochondrial activity and is not inhibited by Bcl2 (Scaffidi et al., 1998). Although recent studies demonstrated that the cleavage of Bid by Casp8 induces the release of cytochrome c and mitochondrial damage in Fas-mediated cell killing (Li et al., 1998; Luo et al., 1998), our data are therefore consistent with the notion that the Fas-mediated PCD pathway can bypass Bcl2/Apaf1/mitochondrial events by directly activating Casp8 at the level of the death receptors. However, in certain types of cells, Fas-induced activation of Casp8 occurs downstream of mitochondrial events (Scaffidi et al., 1998). Moreover, Bcl2 family members have been reported to have inhibitory effects on Fas-induced PCD in some types of cells (Takayama et al., 1995; Armstrong et al., 1996; Boise and Thompson, 1997; Scaffidi et al., 1998). Therefore, it is also possible that the Fas-induced activation of Casp8 observed in *Apaf1*$^{-/-}$ thymocytes is mediated by another Apaf1-like molecule(s), and that the activation of Casp8 is regulated through its association with an Apaf1-like molecule and $BclX_L$ or related molecules (Chinnaiyan et al., 1997).

Role of Apaf1 in a Common PCD Pathway

Apoptosis can be divided into at least three functionally distinct stages: the initiation, effector, and degradation phases (Kroemer et al., 1995). Distinct apoptotic stimuli initiate distinct biochemical events during the heterogeneous initiation phase. However, during the subsequent effector phase, these distinct initiating events are translated into more common events such as the activation of specific caspases. In the degradation phase, phenomena universal to apoptosis induced by all stimuli are observed, including protein degradation, membrane alterations, and DNA cleavage.

The proapoptotic role of Apaf1 previously demonstrated in vitro (Li et al., 1997a; Zou et al., 1997) has been confirmed in vivo and ex vivo in this study. Apaf1-deficient ES cells, EF cells, and thymocytes were remarkably resistant to a wide range of apoptotic stimuli. The apoptotic pathways found in ES and EF cells (and probably neuronal cells) are similar to the apoptotic pathways in *C. elegans* in that they are all dependent on Apaf1 (CED-4). However, our results also show that the dependence of apoptotic pathways on Apaf1 may vary in different types of cells or in different types of tissues or organs, as demonstrated by the differential susceptibility to PCD of ES and EF cells. The broad spectrum of protection evident in Apaf1-deficient cells suggests that Apaf1 plays a critical role in a common pathway, translating and converging different initiating events induced by different apoptotic stimuli into shared effector events. This scenario is reminiscent of the antiapoptotic function of Bcl2, in that Bcl2 blocks apoptosis under a variety of conditions (Hockenbery et al., 1990; Sentman et al., 1991; Korsmeyer, 1992; Reed, 1994).

One model that has been proposed to account for the action of Bcl2 and its antiapoptotic homologs is that these molecules act by stabilizing the mitochondrial membrane and/or preventing the release of cytochrome c from mitochondria. The overexpression of Bcl2 inhibits apoptotic mitochondrial events, including the release of cytochrome c (Kluck et al., 1997; Yang et al., 1997) and the permeability transition (Zamzami et al., 1995; Shimizu et al., 1996). In this model, Apaf1 may work as an activator molecule. In vitro, cytochrome c has been shown to bind to APAF1, causing the activation of CASP9, which in turn activates the key apoptotic enzyme CASP3 (Li et al., 1997a; Zou et al., 1997). It has been reported that cytochrome c release from mitochondria precedes $\Delta\Psi_m$ disruption (Kluck et al., 1997; Yang et al., 1997; Bossy-Wetzel et al., 1998), which is linked to the opening of the PT pores (Kroemer et al., 1997). Moreover, caspases have been shown to directly induce the disruption of $\Delta\Psi_m$ (Susin et al., 1997; Scaffidi et al., 1998). These reports are consistent with the idea that Apaf1 functions in response to the release of cytochrome c by activating caspases and that these caspases can then trigger later mitochondrial damage.

Our finding that $\Delta\Psi_m$ was maintained in *Apaf1*$^{-/-}$ thymocytes is in line with this model and suggests that Apaf1 functions upstream of $\Delta\Psi_m$ and the opening of the PT pores. Moreover, the release of cytochrome c from mitochondria was not impaired in *Apaf1*$^{-/-}$ cells, indicating that Apaf1 acts downstream of cytochrome c release. Thus, a possible sequence of events may entail the release of cytochrome c, which promotes action by Apaf1 to regulate the activation of certain caspases, followed by the caspase-induced proteolytic events including the disruption of $\Delta\Psi_m$ and PT, as has been suggested by Bossy-Wetzel et al. (1998).

Downstream Effectors of Apaf1

What molecules lie immediately downstream of Apaf1? APAF1 has been shown in vitro to interact with CASP4, CASP8, and CASP9 (Li et al., 1997a; Hu et al., 1998; Pan et al., 1998), molecules that contain long prodomains and that are thought to function early in the caspase cascade (Golstein, 1997). Studies in vitro have demonstrated that APAF1 has a stronger affinity for CASP9 than for other caspases, suggesting that in certain situations, the predominant regulatory target of APAF1 is CASP9 (Pan et al., 1998). While *Casp9*$^{-/-}$ EF cells are resistant to various apoptotic stimuli (Hakem et al., 1998), they are invariably more resistant than are *Apaf1*$^{-/-}$ EF cells (H. Y. and T. W. M., unpublished observations). These observations are consistent with a hypothesis that Casp9 is the predominant regulatory target of Apaf1 in EF cells.

Apaf1$^{-/-}$ thymocytes, like *Casp9*$^{-/-}$ thymocytes, showed remarkable resistance to apoptotic stimulations (Hakem et al., 1998; Kuida et al., 1998; and Figure 5). Thymocytes of both mutant mice showed reduced activation of Casp3 in response to these stimulations (Figure 6A). Thus, in thymocytes, Casp9 is likely downstream of Apaf1. However, we have shown in this study that both Casp8 and Casp2 can be regulated downstream of Apaf1. This result indicates that Apaf1 can regulate other caspases in addition to Casp9. Moreover, CASP8 has been shown to interact with CED-4 (Chinnaiyan et al., 1997) or with APAF1 (Hu et al., 1998) through its long prodomain (Hofmann et al., 1997). It is therefore likely that Casp8 lies downstream of Apaf1 and is regulated

via an association with Apaf1. Since recombinant CASP8 was able to activate all known caspases (including CASP1–CASP7, CASP9, and CASP10) in vitro (Srinivasula et al., 1996), it is possible that Apaf1-mediated regulation of Casp8 plays a role in PCD in response to multiple stimuli.

Although the association of Casp2 with Apaf1 has not been proven, Casp2 may also be a downstream effector of Apaf1. Casp2 is classified as an upstream enzyme in caspase cascade, because it has a long prodomain (Kumar et al., 1994). In our experiments, the proteolytic activation of Casp2 was reduced in *Apaf1*$^{-/-}$ thymocytes, suggesting that Casp2 is also downstream of Apaf1. However, it remains possible that the activation of Casp2 and Casp8 is not directly controlled by Apaf1 but is instead regulated by other caspases such as Casp3 or Casp9 (Li et al., 1997b; Hakem et al., 1998).

In summary, our results demonstrate that Apaf1 is crucial for PCD in the developing brain during the embryogenesis. We also show that Apaf1 plays a central role in the common effector phase of mitochondrial PCD pathways in various cell types, possibly by regulating the activation of Casp2, Casp3, and Casp8. However, Fas-induced PCD in thymocytes and activated T cells is independent of Apaf1. Our results also imply the existence of other CED-4/Apaf1-like molecules, the isolation and analysis of which may shed more light on mitochondrial pathways of PCD.

Experimental Procedures

Cells

E14K embryonic stem cells from 129/Ola mice were maintained on a layer of mitomycin C–treated embryonic fibroblasts in Dulbecco's modified Eagle's culture medium (DMEM), supplemented with leukemia inhibitory factor, 15% fetal calf serum (FCS), L-glutamine, and β-mercaptoethanol. *Apaf1*$^{-/-}$ embryonic fibroblasts were obtained from E14.5 embryos and cultured in DMEM supplemented with 5% FCS, L-glutamine, and β-mercaptoethanol.

Generation of *Apaf1*$^{-/-}$ Mutant Mice

Murine *Apaf1* gene fragments were cloned from a 129/J genomic DNA library using a PCR-amplified human *APAF1* cDNA probe. Primers used for amplification of human *APAF1* cDNA commenced at positions 909 and 1321 (5′-GGC CAG TTG TTT TTG TCA A-3′ and 5′-CTG GTT GTA AGA AGA ATC-3′). Five overlapping phage genomic clones containing exons encoding Walker A and Walker B nucleotide-binding P-loop domains (Walker et al., 1982) were isolated. A targeting vector was designed to replace a 4.0 kb genomic fragment containing an exon encoding a portion of the P loop with a neomycin resistance cassette. The neomycin resistance gene (*neo*) was inserted in the targeting vector in the sense orientation to *Apaf1* transcription, such that *neo* was flanked on the 3′ side by 0.8 kb of genomic DNA and on the 5′ side by 4 kb of genomic DNA. The targeting vector was linearized with XhoI and electroporated into E14K ES cells. After G418 selection (200 μg/ml, GIBCO-BRL), homologous recombinants were identified by PCR using a specific primer pair (5′-GGG CCA GCT CAT TCC TC-3′ and 5′-CAC TCT AGT GTC CAG GCT ATC-3′) and confirmed by Southern blotting according to standard protocols. Clones heterozygous for the targeted mutation were injected into 3.5-day C57BL/6 blastocysts, which were subsequently transferred into pseudopregnant foster mothers. Chimeric mice were crossed into strains C57BL/6 or CD1 to produce heterozygous mutant mice. Germline transmission of the mutation was verified by PCR and Southern blot analysis of tail DNA. The null phenotype of *Apaf1*$^{-/-}$ mice was confirmed by Northern blot analysis. Generation of *Apaf1*$^{-/-}$ ES cell lines and *Apaf1*$^{-/-}$/*Rag1*$^{-/-}$ somatic chimeras was performed as described previously (Yoshida et al., 1998).

Histological Analysis

Uteri from plugged females were isolated in ice-cold phosphate-buffered saline at E11.5 to E16.5, fixed overnight in 4% paraformaldehyde at 4°C, dehydrated, and embedded in paraffin. Sections 7 μm thick were cut and stained with thionine.

In Situ Hybridization

For whole-mount in situ hybridization, E9.5 embryos were fixed and processed according to standard protocols. The *Apaf1* probe used was a 400 bp murine cDNA probe synthesized by RT-PCR cloned into the pCRII vector (TA cloning kit, Invitrogen). Probes were synthesized from linearized vector with SP6 or T7 RNA polymerase, labeled with digoxigenin-UTP, and processed as previously described (Hui and Joyner, 1993).

BrdU Labeling of Embryos

BrdU labeling of cells in the S phase of the cell cycle was performed according to the protocol described previously (Hakem et al., 1998). Briefly, BrdU (100 μg/g of body weight) was injected intraperitoneally into pregnant females. The females were sacrificed 1 hr after injection, and the embryos were removed, fixed, dehydrated, and sectioned as for histological analysis. The sections were incubated with an anti-BrdU monoclonal antibody (Becton Dickinson) at a 1:10 dilution. The labeling index (BrdU positive nuclei per total nuclei) was calculated from three serial sections of the mutants and their littermates. At least two mutants were used for each stage of gestation with similar tendency.

Detection of Apoptosis

Detection of apoptosis in the brain was performed by the TUNEL method using the In Situ Cell Death Detection kit (Boehringer Mannheim) according to the manufacturer's directions.

Induction of Apoptosis in ES Cells and EF Cells

To assay PCD of ES cells or EF cells, 1×10^5 cells were plated in each well of a 24-well dish one day prior to treatment. The cells were left untreated or treated with anisomycin (50 μM); etoposide (10 or 100 μM), cisplatinum (10 or 50 μM), or staurosporine (2 or 10 μM) (all from Sigma); or UV irradiation (120 mJ/cm^2) (Stratalinker 2400, Stratagene). After treatment, cells were trypsinized and collected with the supernatants, and cell viability was determined by propidium iodide (PI) and annexin V staining using the Apoptosis Detection Kit (R & D systems) according to the manufacturer's directions. Triplicate samples of each treatment in three independent experiments were assayed.

Immunohistochemistry for the Localization of Cytochrome c

Apaf1$^{+/-}$ or *Apaf1*$^{-/-}$ EF cells were grown on 1 mm glass coverslips for 24 hr and stimulated with etoposide (100 μM), staurosporine (2 μM), or UV irradiation (240 mJ/cm^2). Four hours after stimulation, cells were examined for the intracellular localization of cytochrome c as described elsewhere (Bossy-Wetzel et al., 1998) using anti-cytochrome c antibodies (7H8.2C12, PharMingen) and PI staining.

Induction of Thymocyte Apoptosis

Freshly isolated thymocytes from *Apaf1*$^{-/-}$ mice and their control littermates (10 days old), or *Apaf1*$^{-/-}$/*Rag1*$^{-/-}$ and *Apaf1*$^{+/-}$/*Rag1*$^{-/-}$ somatic chimeric mice (6 to 8 weeks old), were plated in wells of a 48-well dish at 1×10^6 cells/ml in RPMI medium supplemented with 10% FCS. Cells were stimulated with anti-Fas antibody (Jo-2 clone, PharMingen, 1 μg/ml) plus cycloheximide (0–1.0 μg/ml); dexamethasone (1–1000 nM); etoposide (2–50 μM); staurosporine (0.5–10 μM); and γ-irradiation (100–1000 rad), and were stained with PI vs. annexin V (20 hr after stimulation) or $DiOC_6$(3) (6 hr after stimulation) (Molecular Probes) according to the manufacturer's directions.

Assay for Activation-Induced Cell Death

Splenocytes from *Apaf1*$^{-/-}$/*Rag1*$^{-/-}$ and *Apaf1*$^{+/-}$/*Rag1*$^{-/-}$ chimeric mice were stimulated with anti-CD3ε antibody (2 μg/ml) for 24 hr.

Cells were then cultured in 10% Con A-conditioned medium. After 4 days of culture, cells were treated with anti-Fas antibody (1 μg/ml) for 6 or 24 hr, and cell viability was determined by flow cytometry using 7-AAD.

Western Blot Analysis

Thymocytes from newborn mice or *Rag1*$^{-/-}$ chimeric mice were treated for 6 hr with either anti-Fas antibody (1 μg/ml), dexamethasone (5 nM or 1 μM), or etoposide (10 μM). Thymocytes were lysed in 1% NP-40 lysis buffer. Proteins were separated by SDS/PAGE (14% and 10% gels), transferred onto nitrocellulose membranes, and incubated with antibodies reactive to β-actin (Sigma), Casp2 (Santa Cruz), Casp3 (kind gift of R. Sekaly, Montreal, Quebec), or Casp8 (developed in our institute). Optimal antibody concentrations were determined in pilot assays. All immunoblots were visualized by ECL (Amersham).

Acknowledgments

This paper is dedicated to Shirley S.-W. Mak and all victims of breast cancer. We thank A. Wakeham, A. Itie, W. Khoo, A. Hirao, and J. Lam for technical support and animal husbandry; H. Nishina for technical suggestions; J. Henderson for comments on histological analysis of brain; and W.-C. Yeh for critical reading of the manuscript. We also thank M. Saunders for scientific editing and I. Ng for administrative support. Y.-Y. K. and A. H. are supported by a grant from the Medical Research Council of Canada. This work was supported by the National Cancer Institute of Canada and the Medical Research Council of Canada (T. W. M.).

Received June 23, 1998; revised August 6, 1998.

References

Armstrong, R.C., Aja, T., Xiang, J., Gaur, S., Krebs, J.F., Hoang, K., Bai, X., Korsmeyer, S.J., Karanewsky, D.S., Fritz, L.C., and Tomaselli, K.J. (1996). Fas-induced activation of the cell death-related protease CPP32 Is inhibited by Bcl2 and by ICE family protease inhibitors. J. Biol. Chem. *271*, 16850–16855.

Barde, Y.A. (1989). Trophic factors and neuronal survival. Neuron *2*, 1525–1534.

Blaschke, A.J., Staley, K., and Chun, J. (1996). Widespread programmed cell death in proliferative and postmitotic regions of the fetal cerebral cortex. Development *122*, 1165–1174.

Boise, L.H., and Thompson, C.B. (1997). Bcl-x(L) can inhibit apoptosis in cells that have undergone Fas-induced protease activation. Proc. Natl. Acad. Sci. USA *94*, 3759–3764.

Bossy-Wetzel, E., Newmeyer, D.D., and Green, D.R. (1998). Mitochondrial cytochrome c release in apoptosis occurs upstream of DEVD-specific caspase activation and independently of mitochondrial transmembrane depolarization. EMBO J. *17*, 37–49.

Caviness, V.S., Jr., Takahashi, T., and Nowakowski, R.S. (1995). Numbers, time and neocortical neuronogenesis: a general developmental and evolutionary model. Trends Neurosci. *18*, 379–383.

Cecconi, F., Alvarez-Bolado, G., Meyer, B.I., Roth, K.A., and Gruss, P. (1998). Apaf1 (CED-4 homolog) regulates programmed cell death in mammalian development. Cell *94*, this issue, 727–737.

Chinnaiyan, A.M., O'Rourke, K., Lane, B.R., and Dixit, V.M. (1997). Interaction of CED-4 with CED-3 and CED-9: a molecular framework for cell death. Science *275*, 1122–1126.

Clarke, P.G., and Clarke, S. (1996). Nineteenth century research on naturally occurring cell death and related phenomena. Anat. Embryol. (Berl) *193*, 81–99.

Ellis, H.M., and Horvitz, H.R. (1986). Genetic control of programmed cell death in the nematode *C. elegans*. Cell *44*, 817–829.

Fadok, V.A., Voelker, D.R., Campbell, P.A., Cohen, J.J., Bratton, D. L., and Henson, P.M. (1992). Exposure of phosphatidylserine on the surface of apoptotic lymphocytes triggers specific recognition and removal by macrophages. J. Immunol. *148*, 2207–2216.

Fernandes-Alnemri, T., Litwack, G., and Alnemri, E.S. (1994). CPP32, a novel human apoptotic protein with homology to *Caenorhabditis elegans* cell death protein Ced-3 and mammalian interleukin-1 beta-converting enzyme. J. Biol. Chem. *269*, 30761–30764.

Golstein, P. (1997). Controlling cell death. Science *275*, 1081–1082.

Hakem, R., Hakem, A., Duncan, G.S., Henderson, J.T., Woo, M., Soengas, M. S., Elia, A., de la Pompa, J.L., Kägi, D., Khoo, W., Potter, J., Yoshida, R., Kaufman, S.A., Lowe, S.W., Penninger, J.M., and Mak, T. W. (1998). Differential requirement for caspase 9 in apoptotic pathways in vivo. Cell *94*, 339–352.

Hengartner, M.O., and Horvitz, H.R. (1994). *C. elegans* cell survival gene ced-9 encodes a functional homolog of the mammalian proto-oncogene bcl-2. Cell *76*, 665–676.

Hockenbery, D., Núñez, G., Milliman, C., Schreiber, R.D., and Korsmeyer, S.J. (1990). Bcl2 is an inner mitochondrial membrane protein that blocks programmed cell death. Nature *348*, 334–336.

Hofmann, K., Bucher, P., and Tschopp, J. (1997). The CARD domain: a new apoptotic signaling motif. Trends Biochem. Sci. *22*, 155–156.

Horvitz, H.R., Sternberg, P.W., Greenwald, I.S., Fixsen, W., and Ellis, H.M. (1983). Mutations that affect neural cell lineages and cell fates during the development of the nematode *Caenorhabditis elegans*. Cold Spring Harb. Symp. Quant. Biol. *48(2)*, 453–463.

Hu, Y., Benedict, M.A., Wu, D., Inohara, N., and Núñez, G. (1998). Bcl-XL interacts with Apaf-1 and inhibits Apaf-1-dependent caspase-9 activation. Proc. Natl. Acad. Sci. USA *95*, 4386–4391.

Hui, C.C., and Joyner, A.L. (1993). A mouse model of greig cephalopolysyndactyly syndrome: the extra-toesJ mutation contains an intragenic deletion of the Gli3 gene. Nat. Genet. *3*, 241–246.

Jacobson, M.D., Weil, M., and Raff, M.C. (1996). Role of Ced-3/ICE-family proteases in staurosporine-induced programmed cell death. J. Cell. Biol. *133*, 1041–1051.

Jacobson, M.D., Weil, M., and Raff, M.C. (1997). Programmed cell death in animal development. Cell *88*, 347–354.

Kluck, R.M., Bossy-Wetzel, E., Green, D.R., and Newmeyer, D.D. (1997). The release of cytochrome c from mitochondria: a primary site for Bcl2 regulation of apoptosis. Science *275*, 1132–1136.

Korsmeyer, S.J. (1992). Bcl2: a repressor of lymphocyte death. Immunol. Today *13*, 285–288.

Kroemer, G., Petit, P., Zamzami, N., Vayssiere, J.L., and Mignotte, B. (1995). The biochemistry of programmed cell death. FASEB J. *9*, 1277–1287.

Kroemer, G., Zamzami, N., and Susin, S.A. (1997). Mitochondrial control of apoptosis. Immunol. Today *18*, 44–51.

Kuida, K., Zheng, T.S., Na, S., Kuan, C., Yang, D., Karasuyama, H., Rakic, P., and Flavell, R.A. (1996). Decreased apoptosis in the brain and premature lethality in CPP32-deficient mice. Nature *384*, 368–372.

Kuida, K., Haydar, T.F., Kuan, C.-Y., Gu, Y., Taya, C., Karasuyama, H., Su, M.S.-S., Rakic, P., and Flavell, R.A. (1998). Reduced apoptosis and cytochrome c–mediated caspase activation in mice lacking caspase 9. Cell *94*, 325–337.

Kumar, S., Kinoshita, M., Noda, M., Copeland, N.G., and Jenkins, N.A. (1994). Induction of apoptosis by the mouse Nedd2 gene, which encodes a protein similar to the product of the *Caenorhabditis elegans* cell death gene ced-3 and the mammalian IL-1 beta-converting enzyme. Genes Dev. *8*, 1613–1626.

Li, P., Nijhawan, D., Budihardjo, I., Srinivasula, S.M., Ahmad, M., Alnemri, E.S., and Wang, X. (1997a). Cytochrome c and dATP-dependent formation of Apaf-1/caspase-9 complex initiates an apoptotic protease cascade. Cell *91*, 479–489.

Li, H., Bergeron, L., Cryns, V., Pasternack, M.S., Zhu, H., Shi, L., Greenberg, A., and Yuan, J. (1997b). Activation of caspase-2 in apoptosis. J. Biol. Chem. *272*, 21010–21017.

Li, H., Zhu, H., Xu, C.-j., and Yuan, J. (1998). Cleavage of BID by caspase 8 mediates the mitochondrial damage in the Fas pathway of apoptosis. Cell *94*, 491–501.

Luo, X., Budihardjo, I., Zou, H., Slaughter, C., and Wang, X. (1998). Bid, a Bcl2 interacting protein, mediates cytochrome c release from mitochondria in response to activation of cell surface death receptors. Cell *94*, 481–490.

Medema, J.P., Scaffidi, C., Kischkel, F.C., Shevchenko, A., Mann, M., Krammer, P.H., and Peter, M.E. (1997). FLICE is activated by association with the CD95 death-inducing signaling complex (DISC). EMBO J. *16*, 2794–2804.

Muzio, M., Chinnaiyan, A.M., Kischkel, F.C., O'Rourke, K., Shevchenko, A., Ni, J., Scaffidi, C., Bretz, J.D., Zhang, M., Gentz, R., et al. (1996). FLICE, a novel FADD-homologous ICE/CED-3-like protease, is recruited to the CD95 (Fas/APO-1) death-inducing signaling complex. Cell *85*, 817–827.

Nagata, S. (1997). Apoptosis by death factor. Cell *88*, 355–365.

Nicholson, D.W., and Thornberry, N.A. (1997). Caspases: killer proteases. Trends Biochem. Sci. *22*, 299–306.

Oppenheim, R.W. (1991). Cell death during development of the nervous system. Annu. Rev. Neurosci. *14*, 453–501.

Oppenheim, R.W., Prevette, D., Yin, Q.W., Collins, F., and MacDonald, J. (1991). Control of embryonic motoneuron survival in vivo by ciliary neurotrophic factor. Science *251*, 1616–1618.

Pan, G., O'Rourke, K., and Dixit, V.M. (1998). Caspase-9, Bcl-XL, and Apaf-1 form a ternary complex. J. Biol. Chem. *273*, 5841–5845.

Petit, P.X., Lecoeur, H., Zorn, E., Dauguet, C., Mignotte, B., and Gougeon, M.L. (1995). Alterations in mitochondrial structure and function are early events of dexamethasone-induced thymocyte apoptosis. J. Cell. Biol. *130*, 157–167.

Reed, J.C. (1994). Bcl2 and the regulation of programmed cell death. J. Cell. Biol. *124*, 1–6.

Scaffidi, C., Fulda, S., Srinivasan, A., Friesen, C., Li, F., Tomaselli, K. J., Debatin, K.M., Krammer, P.H., and Peter, M.E. (1998). Two CD95 (APO-1/Fas) signaling pathways. EMBO J. *17*, 1675–1687.

Sentman, C.L., Shutter, J.R., Hockenbery, D., Kanagawa, O., and Korsmeyer, S.J. (1991). bcl-2 inhibits multiple forms of apoptosis but not negative selection in thymocytes. Cell *67*, 879–888.

Shaham, S., and Horvitz, H.R. (1996). Developing *Caenorhabditis elegans* neurons may contain both cell-death protective and killer activities. Genes Dev. *10*, 578–591.

Shimizu, S., Eguchi, Y., Kamiike, W., Waguri, S., Uchiyama, Y., Matsuda, H., and Tsujimoto, Y. (1996). Bcl2 blocks loss of mitochondrial membrane potential while ICE inhibitors act at a different step during inhibition of death induced by respiratory chain inhibitors. Oncogene *13*, 21–29.

Shortman, K., Egerton, M., Spangrude, G.J., and Scollay, R. (1990). The generation and fate of thymocytes. Semin. Immunol. *2*, 3–12.

Spector, M.S., Desnoyers, S., Hoeppner, D.J., and Hengartner, M.O. (1997). Interaction between the *C. elegans* cell-death regulators CED-9 and CED-4. Nature *385*, 653–656.

Srinivasula, S.M., Ahmad, M., Fernandes-Alnemri, T., Litwack, G., and Alnemri, E.S. (1996). Molecular ordering of the Fas-apoptotic pathway: the Fas/APO-1 protease Mch5 is a CrmA-inhibitable protease that activates multiple Ced-3/ICE-like cysteine proteases. Proc. Natl. Acad. Sci. USA *93*, 14486–14491.

Surh, C.D., and Sprent, J. (1994). T-cell apoptosis detected in situ during positive and negative selection in the thymus. Nature *372*, 100–103.

Susin, S.A., Zamzami, N., Castedo, M., Daugas, E., Wang, H.G., Geley, S., Fassy, F., Reed, J.C., and Kroemer, G. (1997). The central executioner of apoptosis: multiple connections between protease activation and mitochondria in Fas/APO-1/CD95- and ceramide-induced apoptosis. J. Exp. Med. *186*, 25–37.

Takahashi, T., Nowakowski, R.S., and Caviness, V.S., Jr. (1995). The cell cycle of the pseudostratified ventricular epithelium of the embryonic murine cerebral wall. J. Neurosci. *15*, 6046–6057.

Takayama, S., Sato, T., Krajewski, S., Kochel, K., Irie, S., Millan, J. A., and Reed, J.C. (1995). Cloning and functional analysis of BAG-1: a novel Bcl2-binding protein with anti-cell death activity. Cell *80*, 279–284.

Thornberry, N.A. (1998). Caspases: key mediators of apoptosis. Chem. Biol. *5*, R97-R103.

Walker, J.E., Saraste, M., Runswick, M.J., and Gay, N.J. (1982). Distantly related sequences in the alpha- and beta-subunits of ATP synthase, myosin, kinases and other ATP-requiring enzymes and a common nucleotide binding fold. EMBO J. *1*, 945–951.

Weller, M., Schulz, J.B., Wullner, U., Loschmann, P.A., Klockgether, T., and Dichgans, J. (1997). Developmental and genetic regulation of programmed neuronal death. J. Neural. Transm. Suppl. *50*, 115–123.

Woo, M., Hakem, R., Soengas, M.S., Duncan, G.S., Shahinian, A., Kägi, D., Hakem, A., McCurrach, M., Khoo, W., Kaufman, S.A., et al. (1998). Essential contribution of caspase 3/CPP32 to apoptosis and its associated nuclear changes. Genes Dev. *12*, 806–819.

Wu, D., Wallen, H.D., Inohara, N., and Núñez, G. (1997a). Interaction and regulation of the *Caenorhabditis elegans* death protease CED-3 by CED-4 and CED-9. J. Biol. Chem. *272*, 21449–21454.

Wu, D., Wallen, H.D., and Núñez, G. (1997b). Interaction and regulation of subcellular localization of CED-4 by CED-9. Science *275*, 1126–1129.

Yang, J., Liu, X., Bhalla, K., Kim, C.N., Ibrado, A.M., Cai, J., Peng, T. I., Jones, D.P., and Wang, X. (1997). Prevention of apoptosis by Bcl2: release of cytochrome c from mitochondria blocked. Science *275*, 1129–1132.

Yoshida, H., Nishina, H., Takimoto, H., Marengère, L.E., Wakeham, A.C., Bouchard, D., Kong, Y.Y., Ohteki, T., Shahinian, A., Bachmann, M., et al. (1998). The transcription factor NF-ATc1 regulates lymphocyte proliferation and Th2 cytokine production. Immunity *8*, 115–124.

Yuan, J., Shaham, S., Ledoux, S., Ellis, H.M., and Horvitz, H.R. (1993). The *C. elegans* cell death gene ced-3 encodes a protein similar to mammalian interleukin-1 beta-converting enzyme. Cell *75*, 641–652.

Zamzami, N., Marchetti, P., Castedo, M., Decaudin, D., Macho, A., Hirsch, T., Susin, S.A., Petit, P.X., Mignotte, B., and Kroemer, G. (1995). Sequential reduction of mitochondrial transmembrane potential and generation of reactive oxygen species in early programmed cell death. J. Exp. Med. *182*, 367–377.

Zou, H., Henzel, W.J., Liu, X., Lutschg, A., and Wang, X. (1997). Apaf-1, a human protein homologous to *C. elegans* CED-4, participates in cytochrome c-dependent activation of caspase-3. Cell *90*, 405–413.